One-dimensional time-dependent neutron transport benchmarks

Carol S. Aplin and Douglass L. Henderson

University of Wisconsin, Madison, Department of Nuclear Engineering and Engineering Physics

Introduction

In inertial fusion targets, neutrons born from fusion reactions will interact with the fuel and surrounding materials. Neutrons can also be useful as diagnostic tools for target experiments. Despite these important features, accurate neutron transport codes have yet to be implemented in some radiation hydrodynamics codes. Here we present a quasi-analytic method for solving the one-dimensional neutron transport equation that shows promise for use in radiation hydrodynamics codes. This method also has the near-term use of creating accurate solutions to benchmark problems, allowing for the verification of both deterministic and Monte Carlo neutron transport codes.

Mathematical Development

Infinite Slab

The integral form of the one-speed, one-dimensional, time-dependent neutron transport equation in an infinite slab is [2]

$$\Phi(x,t) = \Sigma_s \int_0^t \int_{-\infty}^{\infty} \frac{e^{-\Sigma v(t-t')}}{2(t-t')} H\left(t-t'-\frac{|x-x'|}{v}\right) \Phi(x',t')dx'dt' + \Phi_0(x,t) \quad (1)$$

where

- Φ is the total scalar flux,
- Φ_0 is the uncollided flux,
- Σ is the neutron scattering plus absorption cross-section,
- Σ_s is the neutron scattering cross-section,
- and v is the neutron speed

Using an external source of $S(x,t) = \frac{S_0\delta(x)\delta(t)}{2}$, the uncollided flux is

$$\Phi_0(x,t) = \frac{S_0}{2}\left(\frac{e^{-\Sigma vt}}{t}\right) H\left(t+\frac{x}{v}\right) H\left(t-\frac{x}{v}\right). \quad (2)$$

The neutrons are confined behind the wavefronts, given by the Heaviside functions $H(t+\frac{x}{v})$ and $H(t-\frac{x}{v})$, figure 1.

The Neumann Series is used to decompose the total flux into a sum of the uncollided and collided fluxes. The source for the n^{th} collided flux is the $(n-1)^{th}$ collided flux. The reduced collision ansatz [3],

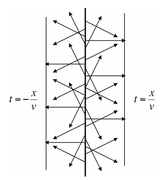

Figure 1: Neutron wavefronts for infinite slab

$$\Phi_n(x,t) = \frac{S_0}{2}\left(\frac{e^{-\Sigma vt}}{t}\right)\left(\frac{(\Sigma_s vt)^n}{n!}\right) F_n(x,t) H(t+\frac{x}{v}) H(t-\frac{x}{v}), \quad (3)$$

is used to obtain an expression for the n^{th} shape factor

$$F_n(x,t)H(t+\frac{x}{v})H(t-\frac{x}{v}) = \frac{n}{2}\int_0^t \int_{-\infty}^{\infty} \frac{dx'dt'}{(t-t')vt'}\left(\frac{(t')^{n-1}}{t^{n-1}}\right) \times F_{n-1}(x',t') H\left(t-t'-\frac{|x-x'|}{v}\right) H(t'+\frac{x'}{v}) H(t'-\frac{x'}{v}) \quad (4)$$

where $F_0 = 1$.

The integration domain is moved into a dimensionless space, figure 2, using a dimensionless time variable, $\eta' = \frac{x'}{vt'}$, and a dimensionless space variable, $\tau' = \frac{t'}{t}$. Implementing this variable transformation, and extracting the Heaviside functions, the n^{th} shape factor, Eq (5) is found. The variable transformation decouples the time and space integrals, allowing the dimensionless time integrals to be performed analytically.

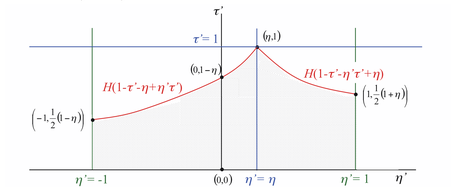

Figure 2: Integration domain for infinite slab

$$F_n(\eta) = \frac{n}{2}\left[\int_{-1}^{\eta}\int_0^{\frac{1-\eta}{1-\eta'}} \frac{(\tau')^{n-1}}{1-\tau'}\frac{\eta'}{\eta} F_{n-1}(\eta')d\tau' d\eta' + \int_{\eta}^{1}\int_0^{\frac{1+\eta}{1+\eta'}} \frac{(\tau')^{n-1}}{1-\tau'}\frac{\eta'}{\eta} F_{n-1}(\eta')d\tau' d\eta'\right] \quad (5)$$

Infinite Sphere

The integral form of the one-speed, one-dimensional, time-dependent neutron transport equation in an infinite sphere is [2]

$$\Phi(r,t) = \Sigma_s \int_0^t \int_0^{\infty} \frac{e^{-\Sigma v(t-t')}}{8\pi r r'(t-t')}\left[H\left(t-t'-\frac{|r-r'|}{v}\right) - H\left(t-t'-\frac{|r+r'|}{v}\right)\right] \Phi(r',t') 4\pi r'^2 dr' dt' + \Phi_0(r,t). \quad (6)$$

Using an external source that is pulsed in space and time, $S(r,t) = \frac{S_0\delta(r)\delta(t)}{4\pi r^2}$, the uncollided flux is

$$\Phi_0(r,t) = \frac{S_0}{4\pi r v t}\left(\frac{e^{-\Sigma vt}}{t}\right)\delta\left(1-\frac{r}{vt}\right). \quad (7)$$

The Neumann Series method is again used to decompose the total flux into a sum of the uncollided and collided fluxes. The spherical coordinates reduced collision ansatz [1] is used to obtain an expression for the n^{th} shape factor:

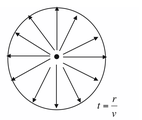

Figure 3: Neutron wavefront for infinite sphere

$$F_n(r,t)H\left(t-\frac{r}{v}\right) = \frac{n}{2}\int_0^t \int_0^{\infty} \frac{dr'dt'}{vt'(t-t')}\left(\frac{t'}{t}\right)^{n-3}\frac{r'}{r} F_{n-1}(r',t') \times H\left(t'-\frac{r'}{v}\right)\left[H\left(t-t'-\frac{|r-r'|}{v}\right) - H\left(t-t'-\frac{|r+r'|}{v}\right)\right]. \quad (8)$$

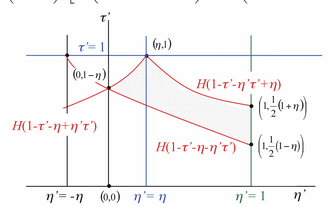

Figure 4: Integration domain for infinite sphere

The variable change to a dimensionless integration space is again utilized:

$$F_n(\eta) = \frac{n}{2}\left[\int_0^{\frac{1-\eta}{1-\eta'}}\int_0^{\eta} \frac{(\tau')^{n-2}}{1-\tau'}\frac{\eta'}{\eta} F_{n-1}(\eta')d\eta' d\tau' + \int_0^{\frac{1+\eta}{1+\eta'}}\int_{\eta}^{1} \frac{(\tau')^{n-2}}{1-\tau'}\frac{\eta'}{\eta} F_{n-1}(\eta')d\eta' d\tau' - \int_0^{\frac{1-\eta}{1+\eta'}}\int_0^{1} \frac{(\tau')^{n-2}}{1-\tau'}\frac{\eta'}{\eta} F_{n-1}(\eta')d\eta' d\tau'\right]. \quad (9)$$

Finite Slab

The same steps for deriving the shape factor for an infinite slab can be followed in deriving the shape factor for a finite slab. After applying the reduced collision ansatz, the following expression is obtained:

$$F_n(x,t)H(t+\frac{x}{v})H(t-\frac{x}{v}) = \frac{n}{2}\int_0^t \int_{-\infty}^{\infty} \frac{dx'dt'}{(t-t')vt'}\left(\frac{(t')^{n-1}}{t^{n-1}}\right) F_{n-1}(x',t') \times H\left(t-t'-\frac{|x-x'|}{v}\right) H(t'+\frac{x'}{v}) H(t'-\frac{x'}{v}) H(b-x') H(b+x') \quad (10)$$

where b is the slab half-width. Due to the boundaries, the Heaviside extraction will result in different expressions for each collision.

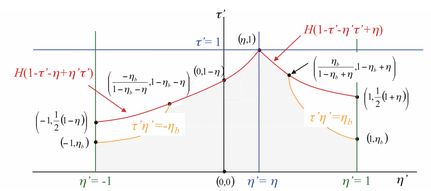

Figure 5: Integration domain for $n=1$ shape factor

where $\eta_b = \frac{b}{vt}$.

The integration domain is the infinite slab integration domain minus the area outside the boundaries. These areas subtracted off create negative neutron sources, or depletion waves.

$$F_1(\eta) = \frac{1}{2}\left[\int_{-1}^{\eta}\int_0^{\frac{1-\eta}{1-\eta'}} F_0(\eta')\frac{d\tau' d\eta'}{1-\tau'} + \int_{\eta}^{1}\int_0^{\frac{1+\eta}{1+\eta'}} F_0(\eta')\frac{d\tau' d\eta'}{1-\tau'} - H(1-2\eta_b-\eta)\int_{-1}^{\frac{-\eta_b}{1-\eta_b-\eta}}\int_{\frac{-\eta_b}{\eta'}}^{\frac{1-\eta}{1-\eta'}} F_0(\eta')\frac{d\tau' d\eta'}{1-\tau'} - H(1-2\eta_b+\eta)\int_{\frac{\eta_b}{1-\eta_b+\eta}}^{1}\int_{\frac{\eta_b}{\eta'}}^{\frac{1+\eta}{1+\eta'}} F_0(\eta')\frac{d\tau' d\eta'}{1-\tau'}\right] \quad (11)$$

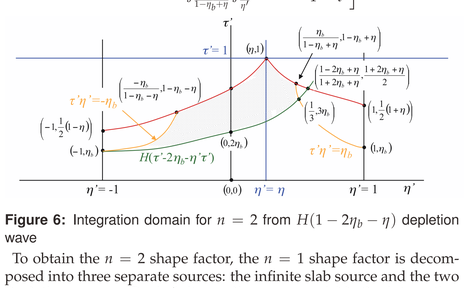

Figure 6: Integration domain for $n=2$ from $H(1-2\eta_b-\eta)$ depletion wave

To obtain the $n=2$ shape factor, the $n=1$ shape factor is decomposed into three separate sources: the infinite slab source and the two depletion waves. The infinite medium source yields the integration domain shown in figure 5. The depletion wave yield the integration domains shown in figures 6 and 7.

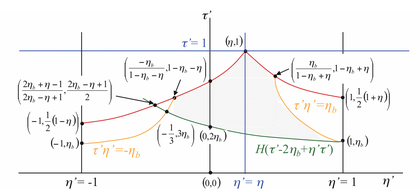

Figure 7: Integration domain for $n=2$ from $H(1-2\eta_b+\eta)$ depletion wave

These two integration domains can be expressed generally as

$$H(1-2\eta_b \mp \eta)\,[Integrals] - H(1-4\eta_b \pm \eta)\,[Integrals]$$

and the integrals have the limits of integration given by figure 6 or 7.

Note that each depletion wave source results in a new depletion wave, in addition to the original depletion wave. Therefore, each collision will produce new depletion waves, with the corresponding integrals to evaluate, in addition to the previous waves already present.

Results

The τ' integrations can be performed analytically and independently of the η' integrations. The η' integrations are performed numerically, using the Gauss-Legendre quadrature rule. Below, results for various benchmark problems are shown for:

- the source strength, S_0, is set to 1
- the neutron speed, v, is set to 1
- the scattering cross section, Σ_s, is set to 1
- the total cross section, $\Sigma = \Sigma_s + \Sigma_a$, is set to 1

Slab Geometry

The infinite and finite slab total fluxes for a pulsed source are shown in figure 8. The infinite slab flux peak decreases with time, and the neutrons are always confined between the wavefronts at $t = \pm\frac{x}{v}$.

Comparing the infinite slab and finite slab fluxes:

- **At 1 mft**: neutrons have not reached the boundary yet, and the infinite and finite medium results match.
- **At 3 mft**: neutrons have started leaking out of the medium. Alternatively, the first depletion waves, $H(1-2\eta_b+\eta)$ and $H(1-2\eta_b-\eta)$, have started crossing the medium, affecting the flux near the boundaries.
- **At 5 mft**: The first depletion waves have almost completely crossed the medium, and the peak finite medium flux separates from the peak infinite medium flux.
- **At 9 mft**: The next set of depletion waves, $H(1-4\eta_b+\eta)$ and $H(1-4\eta_b-\eta)$, begin to cross the medium.

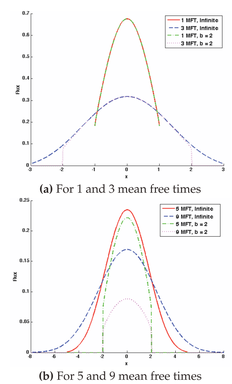

(a) For 1 and 3 mean free times

(b) For 5 and 9 mean free times

Figure 8: Total Flux for Infinite Slab and Finite Slab of half-width $b=2$

Sphere Geometry

Figure 9a shows the total flux for early mean free times for a pulsed source in an infinite spherical medium. The singularity from the uncollided flux is pronounced at early mean free times. Figure 9b shows the total flux at later mean free times. The singularity from the uncollided flux is no longer prominent, and the flux is decaying with time. The neutrons are always confined behind the wavefront at $t = \frac{r}{v}$.

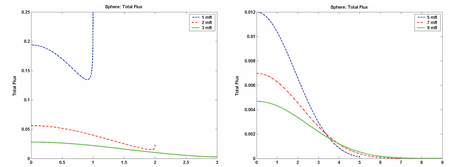

(a) For 1, 2, and 3 mean free times **(b)** For 5, 7, and 9 mean free times

Figure 9: Total Flux for Infinite Sphere

Conclusions

A promising new method for modeling neutron transport has been developed. This method leads to highly accurate solutions, and therefore is useful for producing benchmark results for code verification. With additional features, this method will be useful for modeling neutron transport for inertial confinement fusion systems.

Future Work

The method needs to be expanded to incorporate several more features before it will be appropriate for radiation-hydrodynamics codes used to model inertial confinement fusion implosions. These features include

- Extension to finite sphere geometry
- Heterogeneous media
- Multi-group approximation for energy dependent transport
- Anisotropic scattering

Additionally, we plan to create benchmark solutions to finite slab geometry problems.

References

[1] C. S. Aplin and D. L. Henderson. Time-dependent, one-speed integral transport for one-dimensional infinite media. *Transactions of the American Nuclear Society*, 97:536–539, 2007.

[2] D. L. Henderson and C. W. Maynard. Time-dependent single-collision kernels for integral transport theory. *Nuclear Science and Engineering*, 102:172–182, 1989.

[3] S. A. Kholin. Certain exact solutions of the nonstationary kinetic equation without taking retardation into account. *USSR Computational Mathematics and Mathematical Physics*, 4:213–221, 1964.

Acknowledgments

This work has been performed through grants from the Naval Research Laboratory as part of DOEs funded HAPL program.

My thanks to the Fusion Technology Institute of the University of Wisconsin, Madison, and especially Mohamed Sawan. Also thanks to Greg Moses for his input.